JOURNAL OF THE AMERICAN COLLEGE OF CARDIOLOGY
© 2014 BY THE AMERICAN COLLEGE OF CARDIOLOGY FOUNDATION
PUBLISHED BY ELSEVIER INC.
VOL. 64, NO. 5, 2014
ISSN 0735-1097/$36.00
http://dx.doi.org/10.1016/j.jacc.2014.04.056

Effect of Human Donor Cell Source on Differentiation and Function of Cardiac Induced Pluripotent Stem Cells

Veronica Sanchez-Freire, PhD,*†‡§ Andrew S. Lee, PhD,*†§ Shijun Hu, PhD,*†§ Oscar J. Abilez, MD,† Ping Liang, PhD,*†‡ Feng Lan, PhD,*†‡ Bruno C. Huber, MD,*† Sang-Ging Ong, PhD,*†‡ Wan Xing Hong, MS,*†§ Mei Huang, PhD,*†‡ Joseph C. Wu, MD, PhD*†‡§

ABSTRACT

BACKGROUND Human-induced pluripotent stem cells (iPSCs) are a potentially unlimited source for generation of cardiomyocytes (iPSC-CMs). However, current protocols for iPSC-CM derivation face several challenges, including variability in somatic cell sources and inconsistencies in cardiac differentiation efficiency.

OBJECTIVES This study aimed to assess the effect of epigenetic memory on differentiation and function of iPSC-CMs generated from somatic cell sources of cardiac versus noncardiac origins.

METHODS Cardiac progenitor cells (CPCs) and skin fibroblasts from the same donors were reprogrammed into iPSCs and differentiated into iPSC-CMs via embryoid body and monolayer-based differentiation protocols.

RESULTS Differentiation efficiency was found to be higher in CPC-derived iPSC-CMs (CPC-iPSC-CMs) than in fibroblast-derived iPSC-CMs (Fib-iPSC-CMs). Gene expression analysis during cardiac differentiation demonstrated up-regulation of cardiac transcription factors in CPC-iPSC-CMs, including *NKX2-5*, *MESP1*, *ISL1*, *HAND2*, *MYOCD*, *MEF2C*, and *GATA4*. Epigenetic assessment revealed higher methylation in the promoter region of *NKX2-5* in Fib-iPSC-CMs compared with CPC-iPSC-CMs. Epigenetic differences were found to dissipate with increased cell passaging, and a battery of in vitro assays revealed no significant differences in their morphological and electrophysiological properties at early passage. Finally, cell delivery into a small animal myocardial infarction model indicated that CPC-iPSC-CMs and Fib-iPSC-CMs possess comparable therapeutic capabilities in improving functional recovery in vivo.

CONCLUSIONS This is the first study to compare differentiation of iPSC-CMs from human CPCs versus human fibroblasts from the same donors. The authors demonstrate that although epigenetic memory improves differentiation efficiency of cardiac versus noncardiac somatic cell sources in vitro, it does not contribute to improved functional outcome in vivo. (J Am Coll Cardiol 2014;64:436–48) © 2014 by the American College of Cardiology Foundation.

Coronary heart disease is the leading cause of death in developed countries, accounting for approximately 550,000 deaths annually in the United States alone (1). As the only option for end-stage treatment, heart transplantation excludes many patients who are not suitable candidates because of preexisting comorbidities and is furthermore limited by the low number of available organ donors. In recent years, cell-based

From the *Department of Medicine, Division of Cardiology, Stanford University School of Medicine, Stanford, California; †Stanford Cardiovascular Institute, Stanford University School of Medicine, Stanford, California; ‡Department of Radiology, Stanford University School of Medicine, Stanford, California; and the §Institute of Stem Cell Biology and Regenerative Medicine, Stanford University School of Medicine, Stanford, California. This research was funded by the Swiss National Science Foundation (SNF PBBEP3_129803; Dr. Sanchez-Freire), the German Research Foundation (DFG-Hu-1857/1-1; Dr. Huber), the National Institutes of Health (grants R01HL113006, U01HL099776, P01GM099130, and R24HL117756), the American Heart Association Established Investigator Award 14420025, and the California Institute for Regenerative Medicine (grants DR2-05394 and TR3-05556; Dr. Wu). Drs. Lee and Wu hold shares in Stem Cell Theranostics. All other authors have reported that they have no other relationships relevant to the contents of this paper to disclose.
Listen to this manuscript's audio summary by *JACC* Editor-in-Chief Dr. Valentin Fuster.
You can also listen to this issue's audio summary by *JACC* Editor-in-Chief Dr. Valentin Fuster.

Manuscript received December 23, 2013; revised manuscript received March 31, 2014, accepted April 30, 2014.

therapies have emerged as a promising alternative (2). Human-induced pluripotent stem cells (iPSCs), in particular, are an attractive donor cell source in view of their capacity for unlimited self-renewal and pluripotency (3). In addition, because iPSCs can be derived from various somatic tissue sources (4), their use largely circumvents ethical and immunologic concerns associated with embryonic stem cell (ESC)-based therapies.

SEE PAGE 449

However, several studies have demonstrated that iPSCs are not as similar to ESCs as initially believed (5). Newer published data suggests that epigenetic memory has the potential to influence the differentiation potential and functional maturity of iPSC-derived cell types (6).

In this study, the authors aimed to assess the contributions of epigenetic memory to the differentiation potential, function, and maturity of human iPSCs derived from cardiac and noncardiac sources. To do so, the study generated human iPSCs from cardiac progenitor cells (CPC-iPSCs) and dermal fibroblasts (Fib-iPSCs) from the same donors and differentiated these cells to iPSC-CMs for in vitro and in vivo characterization. Because human CPCs have been shown to give rise to multiple lineages of cells found in the heart (7–9), the authors also compared the ability of CPC-iPSCs and Fib-iPSCs to differentiate into other cell types found in the heart.

METHODS

A detailed Methods section is available in the Online Appendix. Stanford University (Stanford, California) Human Subjects Research Institutional Review Board approved all the protocols in this study. iPSCs were generated using lentiviral transduction, as previously described (4). A modified protocol from Yang et al. (10) was followed to differentiate iPSC-CMs by 3-dimensional (3D) embryoid body (EB) formation. As an alternate method of cardiac differentiation, a 2-dimensional (2D) monolayer protocol from Lian et al. (11) was also used. Following differentiation, iPSC-CMs were cultured in vitro using SCT Cardiac Maintenance Media (Stem Cell Theranostics, Menlo Park, California). A detailed description is included in the Methods section in the Online Appendix.

STATISTICAL ANALYSIS. Normality distribution was studied with the Kolmogorov-Smirnov test ($p < 0.05$). Statistically significant differences were determined using the Mann-Whitney test or Wilcoxon signed rank test, with alpha set to 0.05 for samples not displaying a normal distribution, and with Student *t* test or paired Student *t* test, with alpha set to 0.05 for samples with a normal distribution. Unless specified, data are expressed as mean ± SEM. All statistical analysis was carried out using Prism5 (GraphPad Software, La Jolla, California).

RESULTS

Skin fibroblasts and CPCs were isolated from 2 matched human fetal donors (**Fig. 1A**). To perform CPC isolation, heart tissue was digested to a single cell suspension and labeled with Sca-1 antibody for magnetic cell sorting (12). Following a brief period of cell expansion, fetal CPCs and fibroblasts were characterized for gene expression. Fetal CPCs were found to express genes associated with cardiac lineage, such as *KDR*, *NKX2-5*, *TBX18*, *WT1 MEF2C*, and *GATA4*, whereas fibroblasts expressed only *TBX18* (Online Fig. 1A). Neither the CPCs nor fibroblasts were found to express genes associated with pluripotency such as *NANOG* and *OCT4*, both of which were highly expressed in iPSCs (Online Fig. 1B). CPCs and fibroblasts were subsequently reprogrammed through lentiviral infection using *OCT4*, *SOX2*, *KLF4*, and *c-MYC* (3). After approximately 3 weeks, colonies positive for alkaline phosphatase (**Fig. 1B**) with ESC-like morphology were mechanically isolated and expanded on Matrigel-coated dishes. No differences in reprogramming efficiency were observed between the 2 cell types. Both CPC-iPSCs and Fib-iPSCs exhibited identical morphologies and presence of pluripotency markers such as Tra-1-60, and Oct4 (**Fig. 1B**). Teratoma formation assays using CPC-iPSCs and Fib-iPSCs produced derivatives from all 3 germ layers (**Fig. 1C**). Paired CPC-iPSCs and Fib-iPSCs also were generated from an adult 65-year old donor as an additional control. Reprogramming was conducted in a manner identical to that used in fetal donor sources. Adult CPC-iPSCs and Fib-iPSCs similarly exhibited ESC-like morphologies and markers of pluripotency (Online Fig. 2).

Following iPSC characterization and a brief period of cell expansion, CPC-iPSCs and Fib-iPSCs were differentiated into iPSC-CMs via 3D EB formation (Online Fig. 3A) (10). At day 15 following induction of cardiac differentiation, spontaneously beating EBs were observed under brightfield microscopy. Beating EBs were dissociated into single cells and characterized by confocal microscopy for immunostaining against cardiac-specific markers, such as cardiac troponin T (cTnT) and sarcomeric alpha-actinin (**Fig. 2A**, Online Fig. 3B). A fluorescence-activated cell sorting (FACS) analysis of dissociated EBs confirmed a significantly higher percent of cTnT-positive cells in CPC-iPSC-CMs than in Fib-iPSC-CMs

ABBREVIATIONS AND ACRONYMS

CM = cardiomyocyte
CPC = cardiac progenitor cell
cTnT = cardiac troponin T
EB = embryoid body
EC = endothelial cell
FACS = fluorescence-activated cell sorting
Fib = fibroblast
iPSC = induced pluripotent stem cell
MEA = multielectrode array
MI = myocardial infarction
Sca = stem cell antigen
SMC = smooth muscle cell

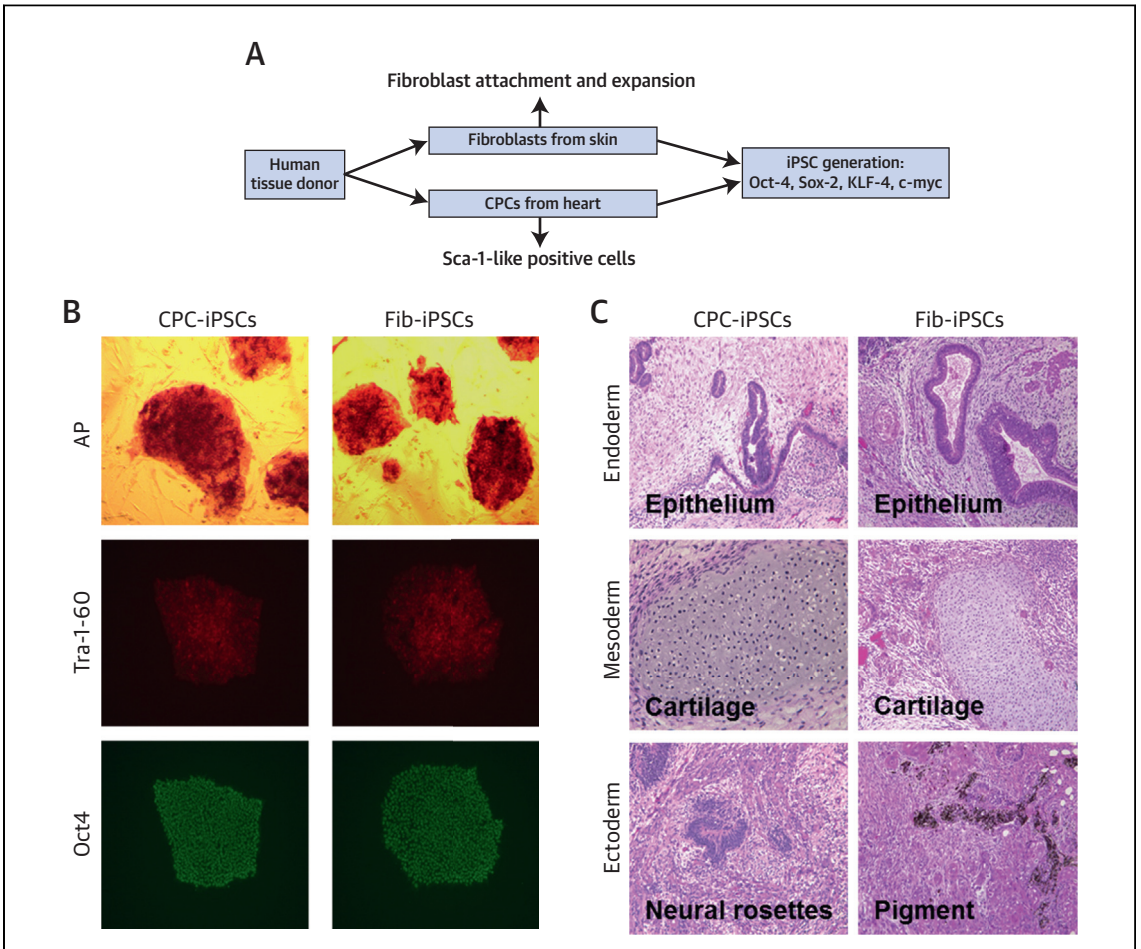

FIGURE 1 **iPSC Generation and Characterization**

(A) Skin fibroblast and cardiac progenitor cell (CPC) primary cultures were established from the same donors and reprogrammed with the pluripotency transcription factors Oct4, Sox2, Klf4, and c-Myc. **(B)** Successfully reprogrammed induced pluripotent stem cells (iPSCs) express standard markers of pluripotency such as alkaline phosphatase (AP), Tra-1-60 **(red)**, and Oct4 **(green)**. **(C)** Following transplantation into immunodeficient mice, CPC-iPSCs and Fib-iPSCs give rise to 3-germ layer teratomas containing endoderm (epithelium), mesoderm (cartilage), and ectoderm (neural rosettes and pigments).

from the same donor (46.2 ± 5.9% vs. 34.0 ± 6.4%, $n = 12$; $p < 0.05$) (Fig. 2B). Quantification of beating EBs at early passage (between 15 and 30) also revealed a higher number of beating EBs for CPC-iPSC-CMs as compared with Fib-iPSC-CMs (40.0 ± 8.9% vs. 19.8 ± 5.2%, $n = 10$; $p < 0.05$) (Fig. 2C), thus indicating higher cardiac differentiation efficiencies for CPC-iPSC-CMs.

To confirm findings that elevated cardiac differentiation efficiency in CPC-iPSC-CMs was not specific to EB-based methods of cardiac differentiation, the authors also utilized a 2D monolayer differentiation protocol on the basis of Lian et al. (Online Fig. 4A) (11). Fetal CPC-iPSC-CMs and Fib-iPSC-CMs generated through monolayer differentiation exhibited the same cardiac markers as iPSC-CMs generated through 3D EB differentiation (Online Fig. 4B). FACS analysis of dissociated monolayers demonstrated a significantly higher percent of cTnT-positive cells in fetal CPC-iPSC-CMs compared with Fib-iPSC-CMs from the same donor (57.2 ± 0.9% vs. 51.7 ± 0.9%, $n = 14$; $p < 0.05$) (Online Figs. 5A and 5B). Immunostaining quantification for cTnT-positive cells using 2D monolayer protocol also revealed significantly higher cardiac differentiation efficiencies for CPC-iPSC-CMs compared with Fib-iPSC-CMs (64.7 ± 1.3% vs. 54.5 ± 1.4%, $n = 20$; $p < 0.05$) (Online Figs. 6A and 6B). Analysis of paired CPC-iPSC-CMs and

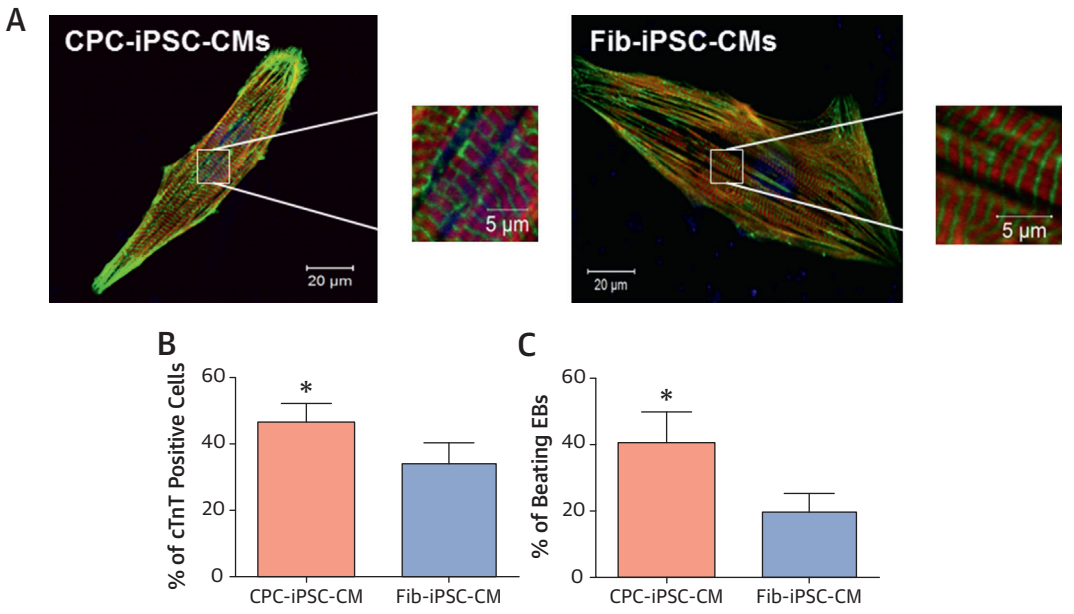

FIGURE 2 Characterization of Induced Pluripotent Stem Cell–Derived Cardiomyocytes

(A) Immunostaining of cardiac progenitor cell-derived induced pluripotent stem cell-derived cardiomyocytes (CPC-iPSC-CMs) and fibroblast-derived induced pluripotent stem cell-derived cardiomyocytes (Fib-iPSC-CMs) for cardiac-specific markers. Pictures show cardiac troponin T **(red)**, sarcomeric alpha-actinin **(green)**, and DAPI **(blue)**. **(B)** Quantification of the percentage of cells positive for cardiac troponin T (cTnT) as determined by fluorescence-activated cell sorting ($n = 12$) at day 15 after cardiac differentiation. The percentage of cTnT positive cells is significantly (*$p < 0.05$) higher in CPC-iPSC-CMs compared with Fib-iPSC-CMs. **(C)** Quantification of the percentage of beating embryoid bodies (EBs) at day 15 post-cardiac differentiation of CPC-iPSCs and Fib-iPSCs ($n = 10$). The percentage of CPC-iPSC beating EBs is significantly higher (*$p < 0.05$) than Fib-iPSC beating EBs.

Fib-iPSC-CMs derived from a 65-year-old adult donor further confirmed results observed in fetal lines. FACS of adult lines demonstrated increased cardiac differentiation for CPC-iPSC-CMs versus Fib-iPSC-CMs ($43.1 \pm 3.7\%$ vs. $35.2 \pm 3.5\%$, $n = 7$; $p < 0.05$) (Online Figs. 7A and 7B). Immunomicroscopy quantification for cTnT-positive cells also yielded similar results in CPC-iPSC-CMs versus Fib-iPSC-CMs ($64.2 \pm 2.7\%$ vs. $45.0 \pm 1.5\%$, $n = 10$; $p < 0.05$) (Online Fig. 8A and 8B). However, prolonged culture of iPSCs for >40 passages negated any differences between CPC-iPSC and Fib-iPSC lines (Online Figs. 9A and 9B). Taken together, these results suggest that at low passages (up to passage 30), derivation of iPSCs from cardiac sources such as CPCs helps enhance the ability of iPSCs to differentiate into cardiac lineages, but this effect is lost with further passage.

During generation of cardiomyocytes from iPSCs, pluripotent cells go through several distinct stages of differentiation, including the creation of an early mesoderm, followed by a cardiac mesoderm specific to different established cardiovascular lineages (10). To improve their understanding of cardiac differentiation in CPC-iPSC-CMs and Fib-iPSC-CMs, the authors grouped specific markers into 1) early cardiac mesodermal transcription factors, 2) cardiovascular progenitor transcription factors, and 3) late-stage cardiogenic transcription factors (Online Fig. 10A). The authors then charted the expression of these markers over the cardiac differentiation process. Specifically, the authors chose *MESP1* as a marker for early cardiac mesoderm, *NKX2-5* and *ISL1* as markers for cardiovascular progenitors, and *HAND2*, *MYOCD*, *TBX5*, *GATA4*, and *MEF2C* as markers for more established cardiac lineages. *MESP1* is a transcription factor necessary for the specification of multipotent cardiovascular progenitors and the expression of cardiovascular transcription factors (13). *HAND2* is a transcription factor involved in heart development (14), whereas *MYOCD* is a transcriptional co-activator of serum response factor (SRF), which interacts with *TBX5* to promote cardiac gene expression (15). *GATA4* is a co-activator of *NKX2-5* (16), a transcription factor involved in heart formation and development (17).

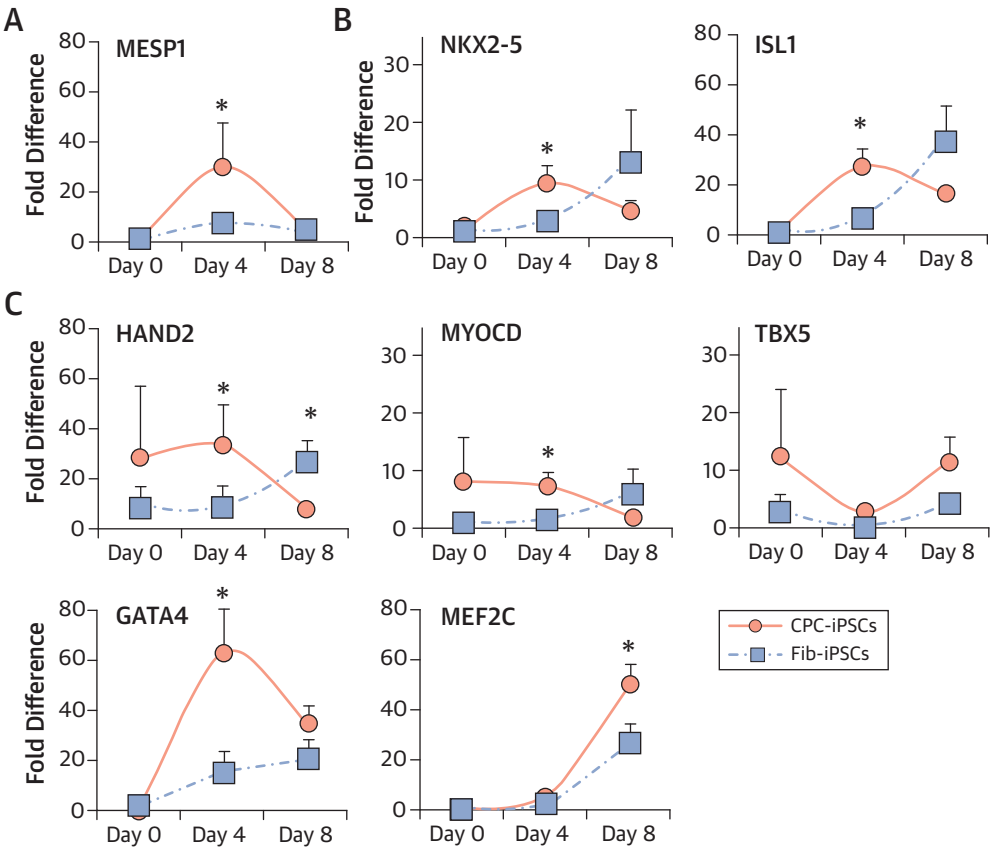

FIGURE 3 Gene Expression Levels During Cardiac Differentiation

Graphs represent expression levels of **(A)** early mesodermal transcription factor, **(B)** early cardiovascular transcription factors, and **(C)** late-stage cardiogenic transcription factors during the process of cardiac differentiation. Gene expression levels are normalized to expression levels in fibroblast-derived induced pluripotent stem cells (Fib-iPSCs) (day 0) to demonstrate expression change over time ($n = 2$ for day 0 and $n = 5$ for day 4 and day 8). *MESP1*, *NKX2-5*, *ISL1*, *HAND2*, *MYOCD*, and *GATA4* levels at day 4 of the cardiac differentiation were significantly higher ($p < 0.05$) in cardiac progenitor cell-derived induced pluripotent stem cells (CPC-iPSCs) than in Fib-iPSCs. At day 8 of the cardiac differentiation, *HAND2* levels were significantly higher ($p < 0.05$) in Fib-iPSCs than in CPC-iPSCs, whereas *MEF2C* levels were significantly higher ($p < 0.05$) in CPC-iPSCs than in Fib-iPSCs.

ISL1 is a transcription factor expressed with *NKX2-5* in cardiac progenitor cells (18), and it is necessary for the formation of the right ventricle (19). Cardiac gene expression was assessed during the differentiation process at day 0 pre-induction, day 4, and day 8 after initiation of differentiation (10). Quantitative polymerase chain reaction demonstrated significantly increased expression of the early cardiac mesodermal marker *MESP1* and of cardiovascular progenitor transcription factors *NKX2-5* and *ISL1* at day 4 of induction in CPC-iPSC-CMs, but not in Fib-iPSC-CMs (**Figs. 3A and 3B**, Online Figs. 10B and 10C). Cardiogenic transcription factors *HAND2, MYOCD,* and *GATA4* were also found to be expressed at significantly higher levels in CPC-iPSCs than in Fib-iPSCs at day 4 of cardiac differentiation (**Fig. 3C**, Online Fig. 10D). By day 8 of induction, only *HAND2* and *MEF2C* presented significant differences. At day 8, *HAND2* was higher in Fib-iPSCs, whereas *MEF2C* was higher in CPC-iPSCs. These findings suggest that the higher efficiency of cardiac differentiation observed for CPC-iPSC-CMs is likely the result of heightened gene expression of cardiac mesodermal and cardiac transcription factors early in the differentiation process.

DNA METHYLATION OF TRANSCRIPTION FACTOR PROMOTER REGION. Several studies have demonstrated that the epigenetic memory of somatic donor cells can result in persistent gene expression, thereby promoting iPSC differentiation toward somatic cell

lineages of origin (20-22). To assess the contribution of epigenetic memory toward differences in gene expression observed during the cardiac differentiation process of CPC-iPSCs and Fib-iPSCs, the authors investigated DNA methylation patterns for the promoter regions of cardiac transcription factors in both cell types. DNA methylation is 1 of several epigenetic mechanisms by which gene regulation is regulated. Methylation of CpGs in the promoter region of a gene typically down-regulates its expression, whereas efficient promoter demethylation of pluripotency genes enhances expression and is necessary for gene reactivation during reprogramming (20,23). Bisulfite sequencing demonstrated higher methylation of a region within 2,000 base pairs immediately upstream of the first coding exon of *NKX2-5* in primary fibroblast cultures and Fib-iPSCs, compared with primary CPC cultures and CPC-iPSCs (**Fig. 4A**). Differences in methylation persisted into day 4 of cardiac differentiation (**Fig. 4B**). The decreased expression of *NKX2.5* found in conjunction with heightened methylation of the *NKX2.5* promoter in Fib-iPSCs suggests that incomplete resetting of the preexisting epigenetic state is a strong contributor to the enriched cardiac gene expression patterns and differentiation efficiencies observed in CPC-iPSCs.

IN VITRO CHARACTERIZATION. Cells generated from iPSCs such as cardiomyocytes are typically developmentally immature in comparison with their adult counterparts (24). Reports have shown that epigenetic memory can improve maturity and function of hematopoietic cells generated from blood cell-derived iPSCs, as compared with iPSCs derived from other cell types (22). The authors therefore assessed whether epigenetic memory from CPC-iPSC generation would result in functional or developmental differences for Fib-iPSC-CMs derived from the same donor. Following completion of cardiac differentiation, electrophysiological properties of CPC-iPSC-CMs and Fib-iPSC-CMs were characterized by calcium (Ca^{2+}) imaging, whole-cell patch clamp, and multi-electrode array (MEA).

Quantification of Ca^{2+} is particularly important because Ca^{2+} is 1 of the major players in excitation-contraction coupling of the heart (25). Furthermore, iPSC-CMs are characterized by immature Ca^{2+} handling properties and incompletely developed sarcoplasmic reticulum (26). To assess whether epigenetic memory contributed toward maturity of CPC-iPSC-CMs, beating EBs were dissociated into single cells or small clumps of CMs for analysis by the Ca^{2+} binding dye Fluo-4 AM. Fluorescence amplitude resulting from Fluo-4 binding to intracellular Ca^{2+} was recorded in both 1 Hz (Online Figs. 11A and 11B) and 2 Hz stimulated beating CMs (Online Figs. 11C and 11D, Online Videos 1 and 2). Peak fluorescence amplitude was roughly the same for both somatic cell sources at 1 Hz and 2 Hz (**Fig. 5A**, Online Videos 1 and 2), indicating that intracellular Ca^{2+} levels were not significantly different between the 2 groups. Other measures of Ca^{2+} handling such as peak rate of Ca^{2+} rise and decline (**Figs. 5B and 5C**), and time

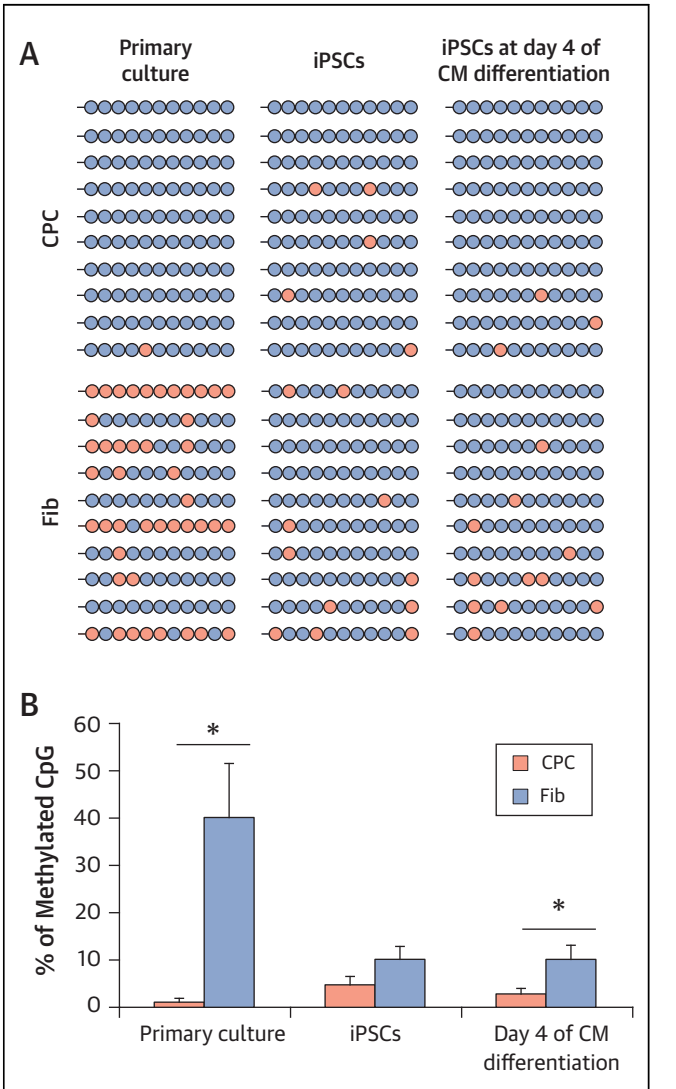

FIGURE 4 Analysis of DNA Methylation Pattern

(A) DNA methylation pattern at the proximal promoter of *NKX2-5* after bisulfite pyrosequencing. **Salmon circles** indicate methylated CpGs, whereas **periwinkle circles** indicate unmethylated CpGs. **(B)** Graph represents the percentage of methylated CpGs in primary cultures, undifferentiated induced pluripotent stem cells (iPSCs), and at day 4 of cardiomyocyte (CM) differentiation from both cardiac progenitor cells (CPCs) and fibroblasts (Fib). Percentage of methylated CpGs is significantly higher in primary fibroblast cultures and in Fib-iPSCs at day 4 of cardiac differentiation.

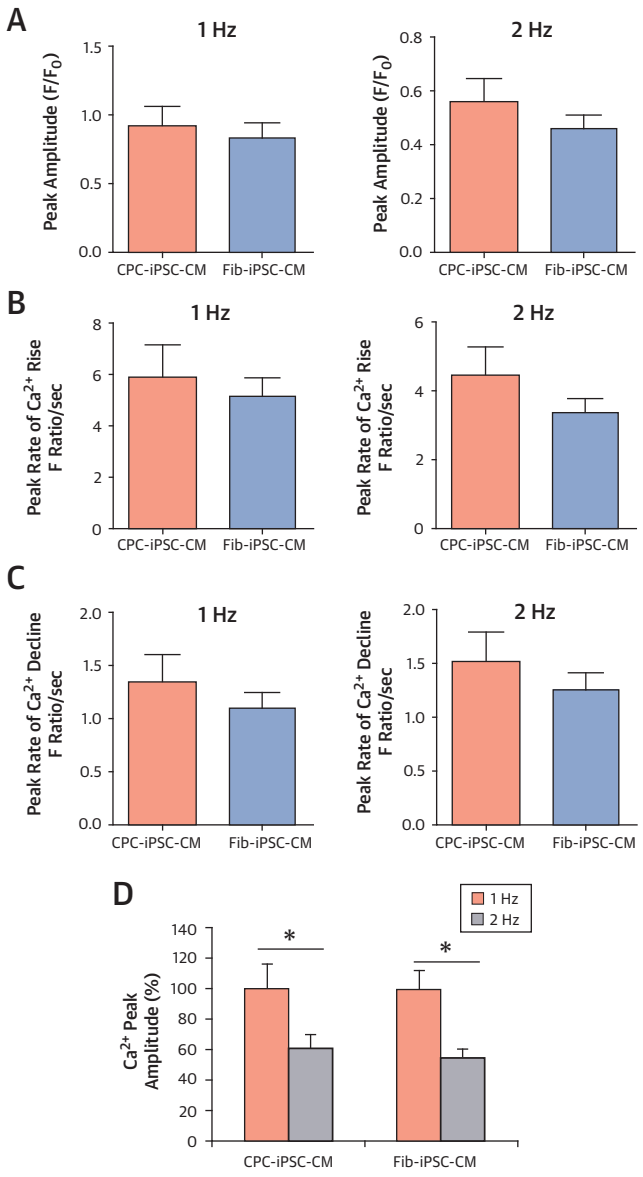

FIGURE 5 Characterization of Intracellular Ca^{2+} Handling

Calcium (Ca^{2+}) handling properties of single cardiomyocytes after Fluo-4 AM imaging at day 28 ± 2 post-differentiation. Cytoplasmic Ca^{2+} levels are directly proportional to fluorescence intensity. **(A)** Quantification of peak amplitude of Fluo-4 AM dye Ca^{2+} transients in cardiac progenitor cell-derived induced pluripotent stem cell-derived cardiomyocytes (CPC-iPSC-CMs) and fibroblast-derived induced pluripotent stem cell-derived cardiomyocytes (Fib-iPSC-CMs) when paced at 1 and 2 Hz (Online Videos 1 and 2). **(B)** Quantification of the peak rate of Ca^{2+} increase in CPC-iPSC-CMs and Fib-iPSC-CMs at 1- and 2-Hz pacing. **(C)** Quantification of peak rate of Ca^{2+} decline presented as fluorescence ratio (F ratio) per second when iPSC-CMs are paced at 1 and 2 Hz. No statistically significant differences were observed between both cell types in any of the studied parameters (CPC-iPSC-CM: n = 20; Fib-iPSC-CM n = 24). **(D)** Graph shows the significant differences between 1 and 2 Hz of the Ca^{2+} peak amplitude in both cell types (CPC-iPSC: 100 ± 16.5% vs 60.6 ± 9.9%, n = 20; Fib-iPSC: 100 ± 12.6% vs 54.7 ± 6.5%, n = 24, $p < 0.05$).

needed to reach 50% and 90% Ca^{2+} decline also did not exhibit any significant differences between CPC-iPSC-CMs and Fib-iPSC-CMs (Online Figs. 11E and 11F). Both CPC-iPSC-CMs and Fib-iPSC-CMs exhibited immature Ca^{2+}-handling properties because increases in beating rate were found to result in significant decreases in cytosolic Ca^{2+} transient amplitudes, a hallmark of developmentally immature cardiac cells (CPC-iPSC: 100 ± 16.5% vs. 60.6 ± 9.9%, n = 20; Fib-iPSC: 100 ± 12.6% vs. 54.7 ± 6.5%, n = 24, $p < 0.05$) (**Fig. 5D**) (27).

ELECTROPHYSIOLOGICAL PROPERTIES. Finally, electrophysiological properties of CPC-iPSC-CMs and Fib-iPSC-CMs were studied using patch clamp and MEA. Beating EBs were dissociated into single cells and seeded on Matrigel-coated coverslips for patch clamp. Action potential (AP) recordings at day 30 ± 2 identified nodal-, atrial-, and ventricular-like CMs among the dissociated cells (**Fig. 6A**). Measurement of key AP parameters, such as the frequency of AP, peak of AP, maximal diastolic potential, AP amplitude, and AP duration, did not uncover statistically significant differences between CPC-iPSC-CM and Fib-iPSC-CM subtypes (**Fig. 6B**). MEA recordings show that spontaneous beating and electrical activity were present in all plated EBs regardless of the somatic cell origin (Online Figs. 12A and 12B, Online Videos 3 and 4). Both CPC-iPSC-CM and Fib-iPSC-CM beating EBs responded to 1 μM of isoproterenol with increased beating frequency (Online Figs. 12C and 12D). Electrophysiological parameters recorded at day 21 ± 2 demonstrated similar mean beating frequencies as indicated by the number of beats per minute (**Fig. 6C**, Online Videos 3 and 4). Baseline field potential duration (FPD) was slightly higher without reaching statistical significance in CPC-iPSC-EBs compared with Fib-iPSC-EBs (**Fig. 6C**). Beating duration suggested that ventricular-like CMs were the predominant cell type in both types of EBs, consistent with single-cell patch clamp data. Taken together, this study's in vitro characterization results show no significant functional differences between CPC-iPSC-CMs and Fib-iPSC-CMs.

ENDOTHELIAL AND VASCULAR SMOOTH MUSCLE DIFFERENTIATION EFFICIENCY. Cardiac progenitor cells give rise not only to CMs, but also to other cell types found normally in the heart (7–9). To investigate whether differences in epigenetic memory could contribute to differentiation into cell fates other than CMs, the authors next differentiated both CPC-iPSCs and Fib-iPSCs into endothelial cell (EC) and vascular smooth muscle cell (SMC) lineages using defined protocols (28,29). For EC differentiation, CD31 was

used as a selection marker (18). FACS analysis revealed that the percent of $CD31^+$ cells resulting from differentiation was significantly higher in CPC-iPSCs when compared with Fib-iPSCs from the same donor (17.2 ± 4.2% vs. 9.7 ± 1.9%, n = 6; $p < 0.05$) (Online Fig. 13A). Immunostaining showed characteristic patterns of CD31 and von Willebrand factor in both CPC-iPSC-ECs and Fib-iPSC-ECs (Online Fig. 13B). For smooth muscle differentiation, alpha-smooth muscle actin (SMA) was used to identify SMCs. FACS analysis demonstrated that CPC-iPSCs produced higher numbers of SMCs than Fib-iPSCs (41.4 ± 8.3% vs. 37.3 ± 8.5%, n = 6; $p < 0.05$) (Online Fig. 14A) when both lines were differentiated in parallel. Immunostaining showed characteristic patterns of alpha-SMA in both CPC-iPSC-SMCs and Fib-iPSC-SMCs (Online Fig. 14B).

ASSESSMENT OF FUNCTIONAL RECOVERY AFTER CELL INJECTION. Because in vitro characterization revealed no significant disparities in CPC-iPSC-CM and Fib-iPSC-CM function, the authors next compared in vivo therapeutic capacity of both cell types in a murine model of myocardial infarction (30). To track survival and engraftment of CPC-iPSC-CMs and Fib-iPSC-CMs in vivo, the authors first transduced CPC-iPSCs and Fib-iPSCs with a lentiviral

A

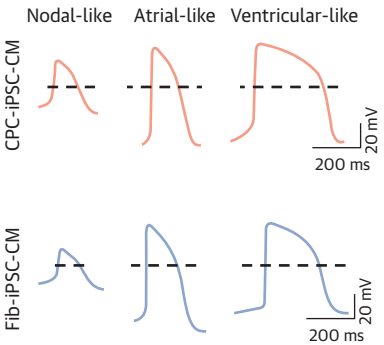

C

	BPM	FPD (ms)
CPC-iPSC-EBs	89.0±23.8	538±69
Fib-iPSC-EBs	85.7±52.6	473±124

B

	% of cells	Frequency of AP (per min)	MDP (mV)	Peak (mV)	APA (mV)	APD_{90} (ms)
CPC-iPSC-CMs						
Nodal-like	3.1	58.0	-38.0	28.7	66.7	205.5
Atrial-like	31.3	28.4±3.2	-45.2±3.2	44.3±4.5	90.5±3.2	245.0±30.0
Ventricular-like	65.6	24.4±4.6	-46.6±4.6	45.4±4.6	92.1±4.6	450.4±37.6
Fib-iPSC-CMs						
Nodal-like	2.7	61.0	-32.0	32.1	64.1	222.0
Atrial-like	29.7	27.5±3.3	-46.9±3.3	44.5±3.3	91.4±4.0	222.4±32.0
Ventricular-like	67.6	25.3±5.0	-46.6±5.0	41.6±5.9	91.0±5.0	427.7±35.0

FIGURE 6 Electrophysiological Characterization of CPC-iPSC-CMs and Fib-iPSC-CMs

(A) Representative action potential (AP) recordings of nodal-, atrial-, and ventricular-like patterns from cardiac progenitor cell-derived induced pluripotent stem cell-derived cardiomyocytes (CPC-iPSC-CMs) and fibroblast-derived induced pluripotent stem cell-derived cardiomyocytes (Fib-iPSC-CMs). **Dashes** indicate 0 mV. **(B)** Comparison of key AP parameters between CPC-iPSC-CMs and Fib-iPSC-CMs. No significant differences in the analyzed parameters were observed between both groups. Values are presented as mean ± SEM (CPC-iPSC-CMs, n = 32; Fib-iPSC-CMs, n = 37). **(C)** Baseline multielectrode array (MEA) electrophysiological parameters for beating embryoid bodies (EBs). Table depicts the comparison between CPC-iPSC-EBs and Fib-iPSC-EBs of beats per minute (BPM) and field potential duration (FPD). Parameters are shown as mean ± SD (n = 10) (Online Videos 3 and 4). APA = action potential amplitude; APD_{90} = action potential duration at 90% repolarization; BPM = beats per minute; FPD = field potential duration; MDP = maximum diastolic potential.

construct driving constitutive expression of firefly luciferase and green fluorescent protein under the control of the ubiquitin promoter. CPC-iPSCs and Fib-iPSCs stably expressing the lentiviral construct were selected by FACS for isolation and expansion. Firefly luciferase expression in sorted CPC-iPSCs and Fib-iPSCs demonstrated no significant differences (Online Figs. 15A and 15B). For delivery into small animal models, approximately 1 million differentiated iPSC-CMs were further enriched by tetramethylrhodamine methyl ester cell sorting and injected into the myocardium of SCID beige mice following ligation of the left anterior descending coronary artery, as previously described (30). Cell engraftment was measured noninvasively by bioluminescence imaging up to 42 days post-surgery (Online Fig. 16). CPC-iPSC-CMs demonstrated mildly higher levels of engraftment as compared with Fib-iPSC-CMs, although both groups exhibited high levels of donor cell death. Assessment of cardiac functional recovery by echocardiography, however, revealed no significant differences between the CPC-iPSC-CM and Fib-iPSC-CM groups at weeks 1, 2, 4, and 8 after MI (**Fig. 7A**). Measurements of the left ventricular wall thickness during systole and diastole did reveal that percentages of left ventricular fractional shortening (LVFS) were not significantly different between CPC-iPSC-CMs and Fib-iPSC-CMs over the 8 weeks, but they were significantly higher in both compared with the phosphate buffered saline control group ($n = 8$; $p < 0.05$) (**Fig. 7B**). The infarction area itself also was assessed with post-mortem triphenyltetrazolium chloride staining (Online Figs. 17A to 17C). Hearts of animals receiving CPC-iPSC-CMs and Fib-iPSC-CMs exhibited smaller infarction sizes than did PBS controls. However, no statistically significant differences

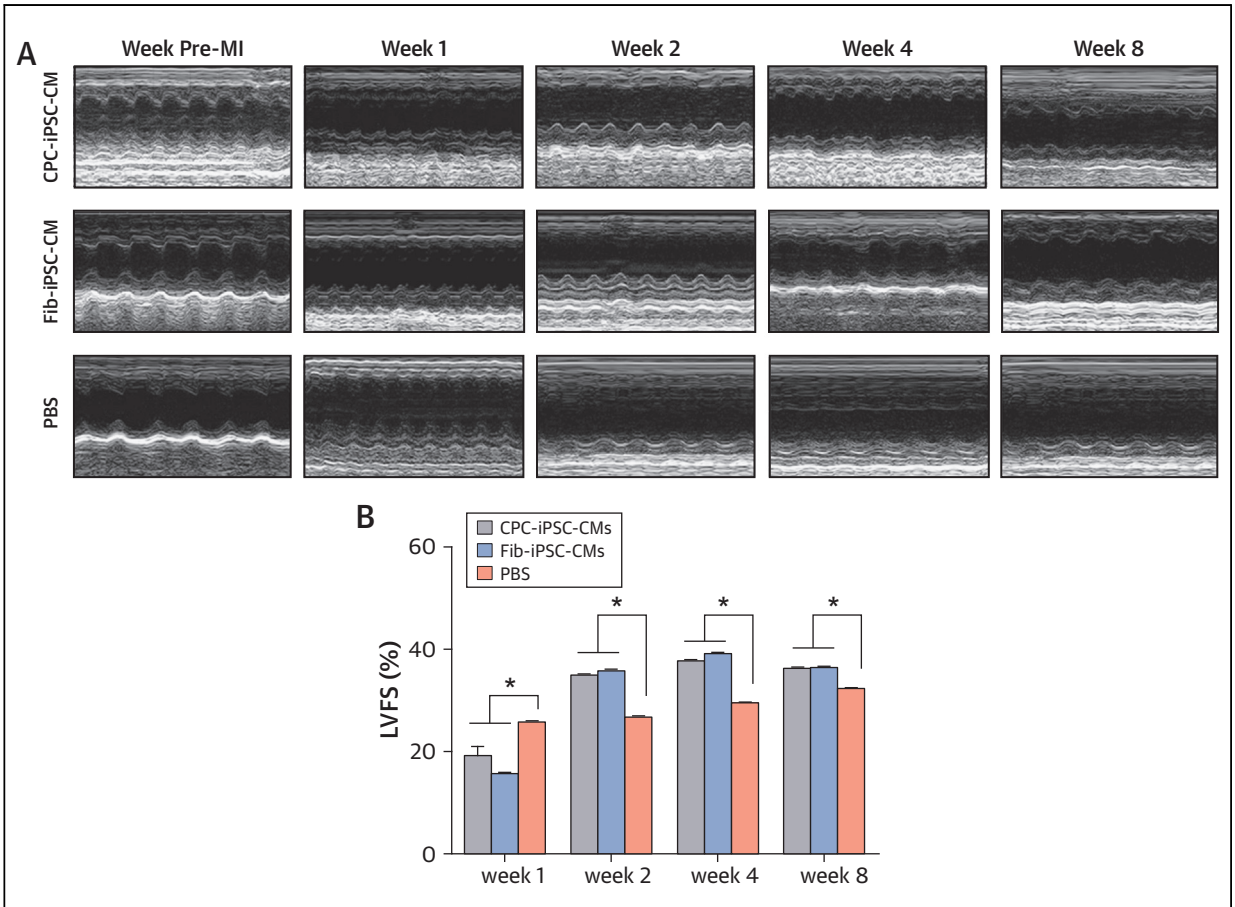

FIGURE 7 Echocardiographic Evaluation of Cardiac Contractility

(A) Representative images of infarcted hearts pre-myocardial infarction (MI) and at weeks 1, 2, 4, and 8 post-infarction. **(B)** Graph shows mean percent of left ventricular fractional shortening (LVFS) for the 3 groups at weeks 1, 2, 4, and 8 post-MI ($n = 8$). PBS = phosphate buffered saline; other abbreviations as in **Figure 2**.

in infarct size were observed between animals receiving CPC-iPSC-CMs and those receiving Fib-iPSC-CMs (infarct size for CPC-iPSC-CMs: 21.9 ± 2.4%, n = 5; Fib-iPSC-CMs: 27.7 ± 3.3%, n = 5; PBS: 42.1 ± 4.2%, n = 3; $p < 0.05$) (Online Fig. 17D).

Taken together, these multiple levels of functional analysis indicate that animals receiving CPC-iPSC-CMs and Fib-iPSC-CMs exhibited greater recovery of cardiac function compared with the PBS controls; however, no significant differences were observed between the CPC-iPSC-CM and Fib-iPSC-CM cohorts.

DISCUSSION

Because cell fate decisions are largely controlled by epigenetic processes, understanding the epigenetic mechanisms underlying stem cell differentiation is crucial for clinical translation of reprogrammed cells. Previous reports demonstrated that perturbation of epigenetic pathways can alter differentiation potential, thereby skewing differentiation toward particular cell lineages and restricting alternative cell fates (20,31,32). Thus, characterization of the epigenetic processes involved in differentiation of pluripotent stem cells to cardiac fate would provide valuable insight into regenerative medicine and drug discovery platforms (2). In this study, the authors demonstrate for the first time that human iPSCs derived from cardiac sources exhibit low levels of methylation on the early mesodermal cardiac promoter *NKX2-5*. These CPC-iPSCs are characterized by earlier and higher expression of cardiac genes that leads to preferential differentiation of cardiac cell fate. Furthermore, the study demonstrates that epigenetic memory of cardiac cell source derivation is eliminated over time (after 40 passages) and does not result in functional differences in vitro or in vivo. These results suggest that differences in CpG methylation in the *NKX2-5* promoter may constitute a crucial mechanism that contributes to different efficiencies observed during cardiac differentiation. Taken together, these findings form a broader understanding of epigenetic regulation of cardiac cell fate and offer a mechanism to improve cardiac differentiation of pluripotent stem cells.

To explain the higher cardiac differentiation efficiency observed in CPC-iPSCs, the authors examined gene expression levels of representative markers from each stage of cardiac differentiation. The markers studied included *MESP1*, *HAND2*, *MYOCD*, *TBX5*, *GATA4*, *MEF2C*, *NKX2-5,* and *ISL1*. Expression levels of cardiovascular progenitor cell markers *NKX2-5* and *ISL1* (17) in particular were found to be significantly higher in CPC-iPSCs at day 4, but not significantly different from Fib-iPSC expression by day 8 of differentiation. The authors believe that the differences in expression of *NKX2-5* and *ISL1* contribute to the disparity in efficiency of cardiac, endothelial, and smooth muscle differentiation in CPC-iPSCs and Fib-iPSCs, particularly in light of the critical role that both genes play in the specification and development of cardiomyocytes.

To elucidate the mechanism underlying the differential expression of transcription factors and cardiac markers, the study compared methylation patterns of *NKX2-5* in CPC-iPSC-CMs and Fib-iPSC-CMs. The analysis focused on the methylation patterns of 11 CpGs within the CpG island located within 2,000 bp upstream of the first exon of *NKX2-5*. Consistent with the gene expression levels presented for primary cultures, the authors observed significantly higher CpG methylation in the original fibroblasts compared with the CPCs. Whereas tissue-specific methylation signatures diminished after reprogramming, silencing remained higher in Fib-iPSCs than in CPC-iPSCs. These findings suggest that certain methylation patterns in iPSCs remain close to the somatic cell types from which they were derived, thus providing evidence of somatic memory after reprogramming (20–22). Furthermore, these results demonstrate that somatic memory in iPSCs is retained during differentiation (21) and therefore can be observed during cardiac differentiation.

Despite differences in methylation and cardiac differentiation efficiency, CPC-iPSC-CMs and Fib-iPSC-CMs were found to exhibit similar sarcomeric structures and in vitro characteristics when assessed by patch clamp, Ca^{2+} handling, and MEA recording. Ca^{2+} handling recordings of both CPC-iPSC-CMs and Fib-iPSC-CMs produced comparable results in all the analyzed parameters. CPC-iPSC-CMs and Fib-iPSC-CMs demonstrated equally immature Ca^{2+}-handling patterns because higher beating frequencies were not accompanied by increases in Ca^{2+} transient amplitude (27). These results point to an immature state of iPSC-CMs, consistent with previous reports (33,34), and they suggest that no residual somatic memory from CPCs contributes to CM maturation, which is a current limitation of iPSC-CMs.

To date, no functional comparison of iPSC-CMs derived from different somatic cell sources from the same human donor has been performed. Using small animal echocardiography, the authors found that the injection of iPSC-CMs improved functional recovery post-MI as compared with animals receiving saline alone. However, significant differences were not observed between mice receiving CPC-iPSC-CMs and those receiving Fib-iPSC-CMs. Taken together, these

results prompt the authors to conclude that although injection of iPSC-CMs improves cardiac function after MI, the somatic source from which iPSC-CMs are derived may not be critical.

STUDY LIMITATIONS. First, as reported in other manuscripts, the therapeutic cells used in this study's animal models of MI were observed to undergo high levels of acute donor cell death following in vivo delivery (35). This finding suggests that long-term functional benefits observed in animals receiving CPC-iPSC-CM and Fib-iPSC-CMs may not be so much the result of persistent donor iPSC-CM integration as a response to the release of paracrine factors in the area of acute ischemic injury (36). Second, the methylation analysis in this study has only a correlative association with the differentiation efficiencies that the authors observed. Methylation assessment demonstrated incomplete silencing of *NKX2-5* in CPC-iPSCs as compared with Fib-iPSCs that, in turn, was associated with higher levels of cardiac gene expression in CPC-iPSCs during the cardiac differentiation process, as well as higher yields of iPSC-CMs. These findings suggest that epigenetic memory contributes to differentiation potential in generation of iPSC-CMs from somatic cell sources, but it does not rule out other regulatory mechanisms of gene expression.

CONCLUSIONS

The authors report for the first time successful generation of iPSCs from CPCs and skin fibroblasts of the same human donors **(Central Illustration)**. Through close observation of iPSC development under directed cardiac differentiation protocols, the study shows that CPC-iPSCs demonstrate a greater efficiency of differentiation into CMs, ECs, and SMCs as compared with Fib-iPSCs at early passage (<30). This is most likely the result of incomplete epigenetic silencing of early cardiac mesodermal transcription factors such as *NKX2-5*. Interestingly, the authors did not observe downstream epigenetic effects on the sarcomere structure, electrophysiological properties,

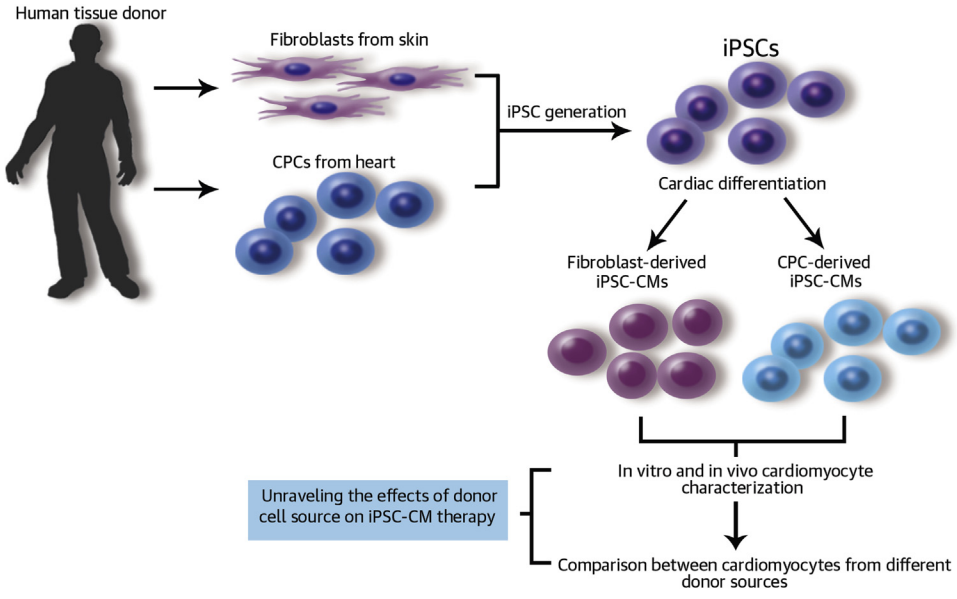

CENTRAL ILLUSTRATION Skin Fibroblast and CPC Primary Cultures Were Established From the Same Human Donors

Somatic cells were reprogrammed into induced pluripotent stem cells (iPSCs) by overexpression of the pluripotency transcription factors Oct4, Sox2, Klf4, and c-Myc. Established iPSCs derived from fibroblasts (Fib-iPSC) and cardiac progenitor cells (CPC-iPSC) were differentiated into cardiomyocytes. Differentiation efficiency was found to be higher in cardiomyocytes derived from CPC-iPSC (CPC-iPSC-CM) compared with Fib-iPSC (Fib-iPSC-CM). In vitro experiments demonstrated that CPC-iPSCs express higher levels of cardiac transcription factors during cardiac differentiation compared with Fib-iPSCs. Epigenetic assessment showed higher methylation in the promoter region of the cardiac transcription factor NKX2-5 in Fib-iPSC-CMs compared with CPC-iPSC-CMs. However, no significant differences in their morphological and electrophysiological properties were observed. In vivo studies using mouse models of myocardial infarction showed comparable therapeutic effects between CPC-iPSC-CM and Fib-iPSC-CM. In summary, whereas epigenetic memory improves cardiac differentiation efficiency in vitro, the in vivo functional recovery following cell transplantation is equivalent.

or restorative function of CPC-iPSC-CMs and Fib-iPSC-CMs in vitro and in vivo. These findings identify an epigenetic regulatory mechanism that is important for differentiation of iPSCs and that may potentially influence future regenerative medicine and drug discovery platforms (2).

ACKNOWLEDGMENTS The authors would like to thank Dr. Enrique G. Navarrete for his assistance with the MEA system. The authors are grateful to Stanford Neuroscience Microscopy Service for assistance with the confocal microscope. They also thank Dr. Joseph Gold for his critical reading of the manuscript.

REPRINT REQUESTS AND CORRESPONDENCE: Dr. Joseph C. Wu, Lorry I. Lokey Stem Cell Research Building, Stanford University School of Medicine, 265 Campus Drive, Room G1120B, Stanford, California 94305-5454. E-mail: joewu@stanford.edu.

PERSPECTIVES

COMPETENCY IN MEDICAL KNOWLEDGE 1: Human iPSCs have unlimited self-renewal and pluripotent properties, and their use also avoids ethical concerns.

COMPETENCY IN MEDICAL KNOWLEDGE 2: Epigenetic memory in human induced human pluripotent stem cells influences the efficiency of cardiac differentiation through regulation of gene expression without appreciably affecting the function of generated cardiomyocytes.

TRANSLATIONAL OUTLOOK: Better understanding of the effects of somatic cell source selection on cardiac differentiation could influence future regenerative medicine and drug discovery platforms.

REFERENCES

1. Go AS, Mozaffarian D, Roger VL, et al. Heart disease and stroke statistics—2013 update: a report from the American Heart Association. Circulation 2013;127:e6–245.

2. Matsa E, Burridge PW, Wu JC. Human stem cells for modeling heart disease and for drug discovery. Sci Transl Med 2014;6:239ps6.

3. Takahashi K, Tanabe K, Ohnuki M, et al. Induction of pluripotent stem cells from adult human fibroblasts by defined factors. Cell 2007;131:861–72.

4. Sun N, Panetta NJ, Gupta DM, et al. Feeder-free derivation of induced pluripotent stem cells from adult human adipose stem cells. Proc Natl Acad Sci U S A 2009;106:15720–5.

5. Narsinh KH, Sun N, Sanchez-Freire V, et al. Single cell transcriptional profiling reveals heterogeneity of human induced pluripotent stem cells. J Clin Invest 2011;121:1217–21.

6. Chang CP, Bruneau BG. Epigenetics and cardiovascular development. Annu Rev Physiol 2012;74:41–68.

7. Beltrami AP, Barlucchi L, Torella D, et al. Adult cardiac stem cells are multipotent and support myocardial regeneration. Cell 2003;114:763–76.

8. Mohsin S, Siddiqi S, Collins B, et al. Empowering adult stem cells for myocardial regeneration. Circ Res 2011;109:1415–28.

9. Matsuura K, Nagai T, Nishigaki N, et al. Adult cardiac Sca-1-positive cells differentiate into beating cardiomyocytes. J Biol Chem 2004;279:11384–91.

10. Yang L, Soonpaa MH, Adler ED, et al. Human cardiovascular progenitor cells develop from a KDR+ embryonic-stem-cell-derived population. Nature 2008;453:524–8.

11. Lian X, Hsiao C, Wilson G, et al. Robust cardiomyocyte differentiation from human pluripotent stem cells via temporal modulation of canonical Wnt signaling. Proc Natl Acad Sci U S A 2012;109:E1848–57.

12. Urbanek K, Torella D, Sheikh F, et al. Myocardial regeneration by activation of multipotent cardiac stem cells in ischemic heart failure. Proc Natl Acad Sci U S A 2005;102:8692–7.

13. Bondue A, Tannler S, Chiapparo G, et al. Defining the earliest step of cardiovascular progenitor specification during embryonic stem cell differentiation. J Cell Biol 2011;192:751–65.

14. Vincentz JW, Barnes RM, Firulli AB. Hand factors as regulators of cardiac morphogenesis and implications for congenital heart defects. Birth Defects Res A Clin Mol Teratol 2011;91:485–94.

15. Wang C, Cao D, Wang Q, Wang DZ. Synergistic activation of cardiac genes by myocardin and Tbx5. PLoS One 2011;6:e24242.

16. Liu Z, Li T, Liu Y, et al. WNT signaling promotes Nkx2.5 expression and early cardiomyogenesis via downregulation of Hdac1. Biochim Biophys Acta 2009;1793:300–11.

17. Scott IC. Life before Nkx2.5: cardiovascular progenitor cells: embryonic origins and development. Curr Top Dev Biol 2012;100:1–31.

18. Moretti A, Caron L, Nakano A, et al. Multipotent embryonic isl1+ progenitor cells lead to cardiac, smooth muscle, and endothelial cell diversification. Cell 2006;127:1151–65.

19. Cai CL, Liang X, Shi Y, et al. Isl1 identifies a cardiac progenitor population that proliferates prior to differentiation and contributes a majority of cells to the heart. Dev Cell 2003;5:877–89.

20. Kim K, Doi A, Wen B, et al. Epigenetic memory in induced pluripotent stem cells. Nature 2010;467:285–90.

21. Lister R, Pelizzola M, Kida YS, et al. Hotspots of aberrant epigenomic reprogramming in human induced pluripotent stem cells. Nature 2011;471:68–73.

22. Kim K, Zhao R, Doi A, et al. Donor cell type can influence the epigenome and differentiation potential of human induced pluripotent stem cells. Nat Biotechnol 2011;29:1117–9.

23. Park IH, Zhao R, West JA, et al. Reprogramming of human somatic cells to pluripotency with defined factors. Nature 2008;451:141–6.

24. Burridge PW, Keller G, Gold JD, et al. Production of de novo cardiomyocytes: human pluripotent stem cell differentiation and direct reprogramming. Cell Stem Cell 2012;10:16–28.

25. Greenstein JL, Winslow RL. Integrative systems models of cardiac excitation-contraction coupling. Circ Res 2011;108:70–84.

26. Fu JD, Li J, Tweedie D, et al. Crucial role of the sarcoplasmic reticulum in the developmental regulation of Ca^{2+} transients and contraction in cardiomyocytes derived from embryonic stem cells. FASEB J 2006;20:181–3.

27. Dolnikov K, Shilkrut M, Zeevi-Levin N, et al. Functional properties of human embryonic stem cell-derived cardiomyocytes: intracellular Ca^{2+} handling and the role of sarcoplasmic reticulum in the contraction. Stem Cells 2006;24:236–45.

28. James D, Nam HS, Seandel M, et al. Expansion and maintenance of human embryonic stem cell-derived endothelial cells by TGFbeta inhibition is Id1 dependent. Nat Biotechnol 2010;28:161–6.

29. Ge X, Ren Y, Bartulos O, et al. Modeling supravalvular aortic stenosis syndrome with human induced pluripotent stem cells. Circulation 2012;126:1695–704.

30. Liu J, Narsinh KH, Lan F, et al. Early stem cell engraftment predicts late cardiac functional recovery: preclinical insights from molecular imaging. Circ Cardiovasc Imaging 2012;5:481–90.

31. Bar-Nur O, Russ HA, Efrat S, et al. Epigenetic memory and preferential lineage-specific differentiation in induced pluripotent stem cells derived from human pancreatic islet beta cells. Cell Stem Cell 2011;9:17–23.

32. Polo JM, Liu S, Figueroa ME, et al. Cell type of origin influences the molecular and functional properties of mouse induced pluripotent stem cells. Nat Biotechnol 2010;28:848–55.

33. Liu J, Fu JD, Siu CW, et al. Functional sarcoplasmic reticulum for calcium handling of human embryonic stem cell-derived cardiomyocytes: insights for driven maturation. Stem Cells 2007;25:3038–44.

34. Itzhaki I, Rapoport S, Huber I, et al. Calcium handling in human induced pluripotent stem cell derived cardiomyocytes. PLoS One 2011;6:e18037.

35. Li Z, Lee A, Huang M, et al. Imaging survival and function of transplanted cardiac resident stem cells. J Am Coll Cardiol 2009;53:1229–40.

36. Gu M, Nguyen PK, Lee AS, et al. Microfluidic single-cell analysis shows that porcine induced pluripotent stem cell–derived endothelial cells improve myocardial function by paracrine activation. Circ Res 2012;111:882–93.

KEY WORDS cardiac differentiation, DNA methylation, epigenetic memory, pluripotent stem cells

APPENDIX For a supplemental Methods section, figures, tables, and videos, please see the online version of this article.